Journal of Instrumentation

Refining and testing 12,000 km of scintillating plastic fibre for the LHCb SciFi tracker

Jinst

Published by IOP Publishing for Sissa Medialab

Received: *July 18, 2018*
Accepted: *October 8, 2018*
Published: *October 19, 2018*

Refining and testing 12,000 km of scintillating plastic fibre for the LHCb SciFi tracker

A.B.R. Cavalcante,[a,1] **B. Dey,**[b] **L. Gavardi,**[c] **L. Gruber,**[d,2] **C. Joram,**[d] **R. Kristic,**[d] **O. Shinji**[e] **and V. Zhukov**[f]

[a] *CBPF,*
Rio de Janeiro, Brazil
[b] *CCNU,*
Wuhan, China
[c] *Technische Universität Dortmund,*
D-44221 Dortmund, Germany
[d] *CERN, EP Department,*
CH-1211 Geneva 23, Switzerland
[e] *Kuraray CO., LTD., Methacrylate Development Department,*
Tokyo, 100-8115, Japan
[f] *RWTH,*
Aachen, Germany

E-mail: lukas.gruber@cern.ch

Abstract: The LHCb Collaboration is constructing a large scintillating fibre tracker for a major upgrade of the experiment during the LHC long shutdown LS2 scheduled for 2019–2020. The detector is based on blue emitting Kuraray SCSF-78MJ fibres of 0.25 mm diameter, read out by linear 128-channel Hamamatsu SiPM arrays. Over a period of about 2 years the full supply of 12,000 km of fibres underwent a systematic and rigorous quality assurance program, including geometrical refinement to deal with rare punctual imperfections. The measurements comprised attenuation length, ionisation light yield, diameter, cladding integrity and radiation tolerance to X-rays. The supply was found to be timely and of very high quality and stability, which led to negligible rejection rates. A small but systematic degradation of the attenuation length by about 1.4% per year is interpreted as natural aging due to oxidation of the polystyrene fibre core and is subject of further investigations.

Keywords: Large detector systems for particle and astroparticle physics; Particle tracking detectors; Scintillators, scintillation and light emission processes (solid, gas and liquid scintillators)

[1] Now at EPFL, Lausanne, Switzerland.
[2] Corresponding author.

https://doi.org/10.1088/1748-0221/13/10/P10025

2018 JINST 13 P10025

Contents

1 Introduction

The LHCb experiment is currently preparing for a major upgrade in order to run from 2021 onwards at a five times higher luminosity of $2 \times 10^{33}\,\mathrm{cm}^{-2}\mathrm{s}^{-1}$ and a readout rate of 40 MHz (bunch crossing every 25 ns). As a part of the ambitious upgrade program, the current outer and inner trackers, consisting of straw tubes and silicon micro strip detectors, respectively, are going to be replaced by a single detector technology, a large scintillating fibre (SciFi) tracker [1, 2].

The SciFi tracker consists of three tracking stations with four individual planes each (X-U-V-X, U and V with ±5° stereo angle) with a size of about $6 \times 4.8\,\mathrm{m}^2$ (see figure 1), resulting in a total detection area of about $340\,\mathrm{m}^2$. The active surface consists of more than 10,000 km of scintillating plastic fibre (12,000 km including spares) with a circular cross section and a diameter of 250 μm. The fibres are arranged in a 6-layer staggered pattern with 275 μm pitch to form 1.35 mm thick fibre mats. The 1024 mats are 2.4 m long and 13 cm wide. They are read out at one end by linear 128-channel arrays of SiPM detectors, while the other end, which is located at the level of the LHC beam axis, is mirrored. Each fibre mat is equipped with four SiPM arrays resulting in a total of about 520k SiPM channels. The trigger-less readout occurs through custom-designed front-end electronics at a rate of 40 MHz.

2018 JINST 13 P10025

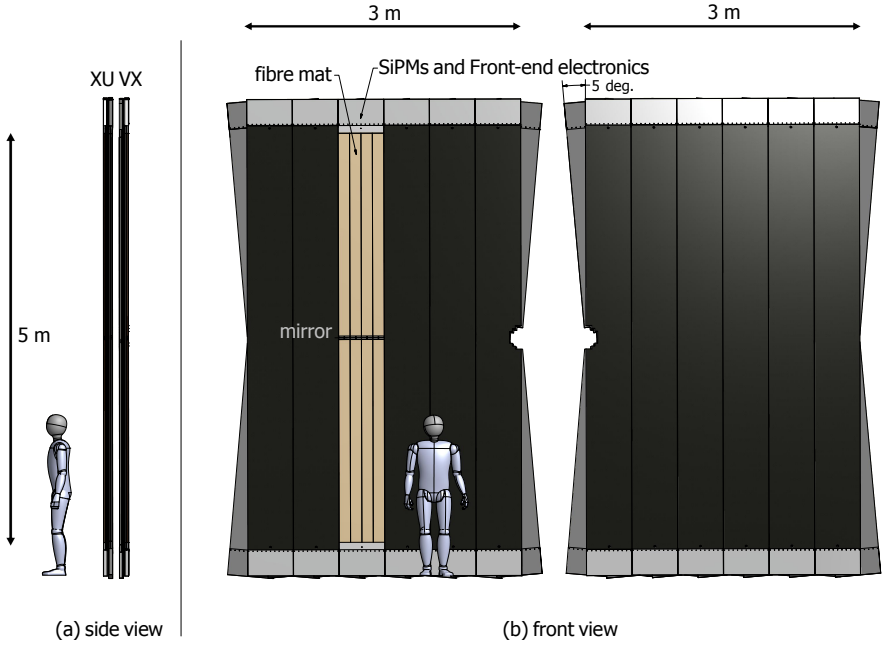

Figure 1. SciFi tracking station, shown in a semi-open configuration.

The SciFi tracker requires a hit detection efficiency of 99%, a spatial resolution better than 100 µm in the horizontal bending plane and a low material budget ($X/X_0 \leq 1\%$). Because of the harsh radiation environment in LHCb, the main challenge is to maintain the aforementioned performance parameters until the end of the foreseen detector lifetime, after 10 years of operation and 50 fb^{-1} integrated luminosity. In order to fulfil these demands the SciFi tracker requires high quality scintillating fibres with small diameter. In particular, the attenuation length should be long (> 3 m), the intrinsic ionisation light yield as high as possible and the fibres should be moderately radiation hard, since close to the beam pipe an ionising dose of 35 kGy is expected. In addition, the geometrical quality of the fibres plays a crucial role. Especially the presence of diameter variations would distort the fibre mat pattern and lead to reduced efficiency and spatial resolution. Therefore these imperfections need to be located and eliminated.

The layout of this article is as follows. It first discusses the challenges and requirements as well as the technical specifications of the scintillating fibres for the SciFi tracker. It then describes the technical and experimental methods, which were used to systematically test and verify the quality of 12,000 km of scintillating fibres. The quality assurance (QA) procedure included measurements of the attenuation length, ionisation light yield, resistance to X-rays and minimum bending radius for a large number of fibre samples. In addition, a dedicated fibre scanning machine precisely monitored the diameter and cladding integrity of the fibres at high throughput. In this context a novel method was developed to refine the geometrical quality of the fibres by removing diameter defects ("bump shrinking"). Finally, the obtained results are presented and discussed and these are followed by conclusions.

2018 JINST 13 P10025

2 Scintillating fibres for the LHCb SciFi tracker

Blue emitting plastic scintillating fibres of type SCSF-78MJ with 250 μm diameter produced by Kuraray were chosen for the LHCb SciFi tracker.[1] The producer states an attenuation length of at least 4 m for 1 mm non-S-type fibres and an intrinsic ionisation light yield of 8,000 photons per MeV energy deposit. In non-S-type fibres the styrene chains are randomly oriented while they are aligned along the fibre axis in S-type fibres. The S-type fibres are mechanically stronger, however show a reduced attenuation length. Fibres of 0.25 mm diameter are produced only in a single quality which corresponds to semi-S-type. The fibres are made from a polystyrene (PS) core (refractive index $n = 1.59$), surrounded by a double cladding structure of polymethylmethacrylate (PMMA, $n = 1.49$) and a fluorinated polymer ($n = 1.42$). The thickness of each cladding layer is 3% of the total fibre diameter. To overcome the poor intrinsic scintillation light yield of PS, the core is doped with an activator and a wavelength shifter (WLS) dye. Their identity and concentrations are not disclosed by the supplier, but have to be carefully tuned to maximise light yield and attenuation length.

The transport of light along the fibre is based on total internal reflection. The used fibre type achieves a trapping efficiency of 5.3% per hemisphere. As the light travels along the fibre, it is attenuated by Rayleigh scattering (due to small density fluctuations), self-absorption by the WLS, radiation induced defects or other losses at the different interfaces (core — cladding — air). The light attenuation can be characterised by the wavelength dependent attenuation length $\Lambda(\lambda)$ and the intensity at a certain distance x along the fibre can be approximated by an exponential, $I(x, \lambda) = I_0 \exp[-x/\Lambda(\lambda)]$. The SCSF-78MJ fibre has its maximum emission at a wavelength of $\lambda = 430$ nm. However, the effective emission spectrum at the end of the fibre is shifted towards the red due to stronger absorption and scattering effects at shorter wavelengths. This effect becomes especially important when using long scintillating fibres, as it is the case for the SciFi tracker. The emission spectrum at the end of the fibre should be optimally matched to the spectral photodetection efficiency (PDE) of the photodetector. On the left hand side of figure 2 the emission spectrum of the SCSF-78MJ fibre is shown for different distances between the excitation point and a spectrometer. The plot on the right hand side shows the spectral attenuation length of SCSF-78MJ, compared to various other blue and green emitting fibres, including the NOL prototype fibres mentioned below. Details about the attenuation length measurement are given in section 3.

In LHCb, the transparency of the fibres will degrade due to the high ionising dose with an expected maximum of 35 kGy close to the beam pipe. This is however the region furthest from the photodetectors and where most of the interesting signal events will occur. The produced light has to travel up to 2.4 m, the reflected photons even up to twice this distance. Therefore attenuation length and intrinsic light yield should be as high as possible. For a non-irradiated fibre, a value of $\Lambda = 3$ m, averaged over the emission spectrum, is considered as lower limit. The light yield limit is discussed later in more detail.

Several irradiation campaigns were performed and predict a signal loss of about 40% for the most irradiated regions at the end of the tracker's lifetime [3]. At the position of the SiPMs, the ionising dose is relatively low (50 Gy) and the main concern will be the neutron fluence of up to 6×10^{11} neq/cm^2 and the associated increase in leakage current, i.e. dark count rate. In order to keep the rate of dark counts at an acceptable level the photodetector arrays are cooled to −40°C. The

[1] Kuraray Co. Ltd., Tokyo, Japan, http://kuraraypsf.jp/psf/.

2018 JINST 13 P10025

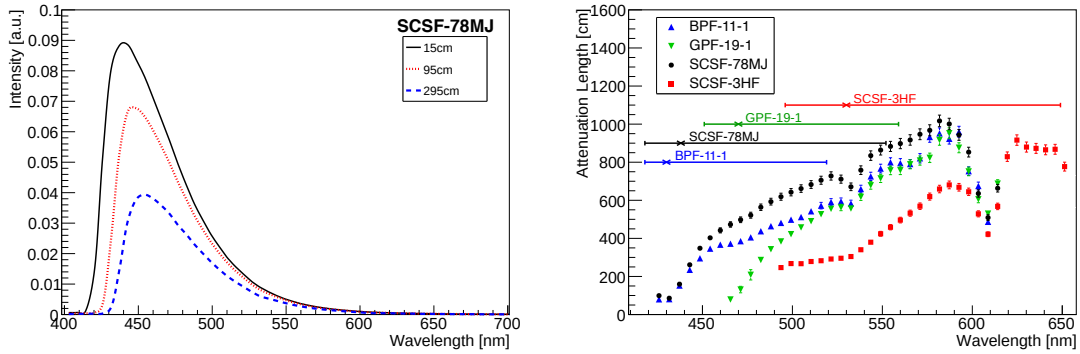

Figure 2. Left: emission spectrum at three different distances from a spectrometer for Kuraray SCSF-78MJ. Right: wavelength dependent attenuation for Kuraray fibres (SCSF-78MJ and SCSF-3HF) and NOL fibres (BPF-11-1 and GPF-19-1). The horizontal lines indicate the emission range, the wavelength of maximum emission is marked by an x.

detectors are housed in gas- and light-tight boxes, which are flushed by dry air (dew point −70°C) to avoid condensation.

Initially, the SciFi tracker will yield about 18–20 photoelectrons (p.e.) per detector plane for particles hitting close to the beam pipe. At the end of the lifetime, the measured light output will still be well above 10 p.e., which will allow for a detection efficiency of 99% as well as a resolution better than 100 µm. A recent study [4] aims at the development of scintillating fibres with very short decay time and high light yield, which are based on a novel type of luminophores (NOL) admixed to the PS core.[2] The fibres are expected to be similarly affected by radiation as the standard material but may benefit from an initially higher light yield and might be interesting for a future upgrade or replacement of the innermost regions of the SciFi tracker.

The verification of the fibre diameter (nominally 250 µm) and its uniformity is an integral part of the QA. The control of the diameter of such thin fibres is a challenge for the producer. During production, the fibre diameter is measured on-line and the acquired information is fed back to the control of the drawing speed. Fine tuning of the control loop parameters minimises the periodic diameter variations which are typically at length scales of meters with an amplitude in the order of a few % of the nominal fibre diameter. However there are also diameter fluctuations that appear at much smaller length scales, typically cm or mm, which are caused by the inclusion of solid (e.g. glass) or soft materials (e.g. dust) or non-uniformities in the core and cladding materials. Such defects are usually referred to as "bumps" (diameter increase) or "necks" (diameter decrease). Despite a clean work environment and other process optimisations, the occurrence of such defects could not be fully avoided during production. The bump (over-)size can range from a few % of the nominal diameter to several fibre diameters. Bumps or necks cause deficits in the light transport (light leaks) of a fibre and potentially reduce its mechanical stability. In the SciFi tracker, bumps lead to distortions in the 6-layer pattern of the fibre mats, affecting hit efficiency and position resolution. Empirically, defects with a diameter larger than 350 µm tend to cause irregular winding patterns

[2]NOL = Nanostructured Organo-silicon Luminophore. In NOL fibres, activator and wavelength shifter complexes are arranged in close distance.

2018 JINST 13 P10025

and complicate or delay the fibre mat winding. A dedicated fibre scanning machine was built to monitor the fibre diameter and cladding integrity. The scanner automatically detected bumps and necks and precisely recorded their shape. As described below in more detail, bumps exceeding a diameter of 350 µm were shrunk by drawing the fibre through a hot conical tool.

3 Fibre quality assurance

The fibre production was organised in three phases: (1) a 500 km pre-series, (2) a 10,500 km main series and (3) 1,000 km spare fibres. After the pre-series, a six-weeks delay allowed for an in-depth qualification before the start of the main series. The supply was divided into 48 individual shipments (batches) arriving at CERN in weekly (100 km) or bi-weekly (300 km) intervals. The fibres were supplied on plastic spools of 210 mm core diameter, with typically 12.5 km length. After arrival, the necessary fibre samples for QA were prepared and the individual fibre spools were processed on the fibre scanner.

The following sections describe the individual experimental methods which are part of our fibre QA procedure and performed for all fibres received from Kuraray in a standardised and repetitive manner. For each step we give a short description of the experimental set-up and results of a typical measurement.

3.1 Attenuation length

In order to determine the attenuation length of a scintillating fibre, its wavelength shifter dye is excited by passing the fibre through an integrating sphere-like cavity which houses an arrangement of four UV-LEDs (390 nm) that can be moved along the length of the fibre. One fibre extremity is read out by a Si-PIN photodiode (Newport 818-UV), while the other end is painted black to avoid Fresnel reflection of the light back into the fibre. A schematic of the experimental set-up is shown in figure 3. It is described in more detail in ref. [5]. To extract the integral attenuation length Λ, the measured light intensity is recorded as a function of the excitation position x and fitted with a single exponential function of the form $I = I_0 \exp(-x/\Lambda)$, where I_0 is the intensity at zero distance.

The fit range is chosen between 100 cm and 300 cm from the photodiode end to avoid the contribution of a second exponential with shorter attenuation length, due to light losses inside the cladding and photons travelling on non-meridional paths inside the fibre. Typical values for the short exponential term are in the order of a few tens of cm, such that the steep component is already sufficiently attenuated at 100 cm. Another reason is that also Kuraray uses the same fit limits to determine the attenuation length of all fibres prior to delivery. However it should be noted that the so-determined integral (i.e. not wavelength resolved) attenuation length depends on the spectral sensitivity of the chosen photodetector and therefore may not be directly comparable with other measurements. Figure 4, right, shows a typical measurement of the attenuation length of a SCSF-78 fibre from the main series production.

3.2 Ionisation light yield

The determination of light yield in the context of the QA relies on a relative comparison of fibre samples under well defined and reproducible experimental conditions, as the measurement of the intrinsic ionisation light yield of thin scintillating fibres would require knowledge of many

2018 JINST 13 P10025

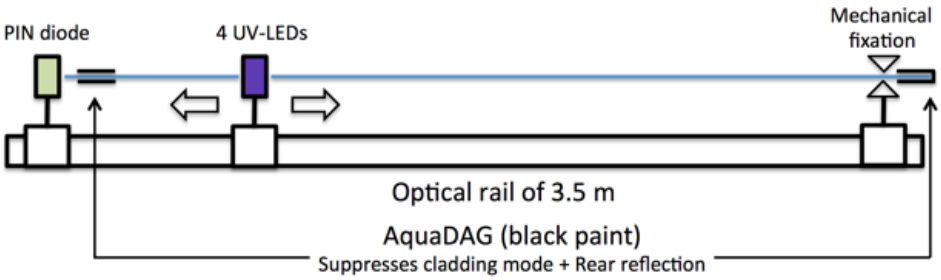

Figure 3. Illustration of the experimental set-up used for attenuation length measurements.

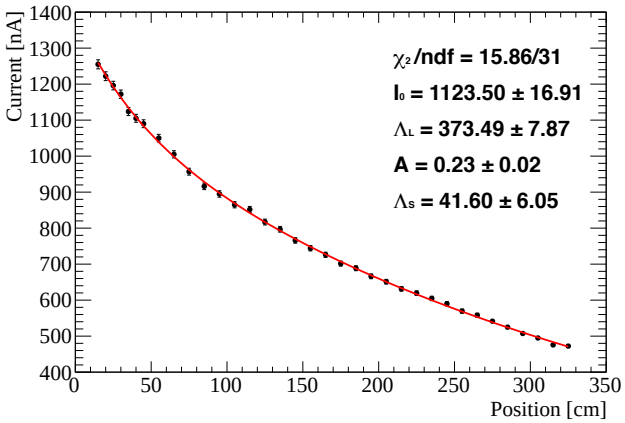

Figure 4. Example attenuation length measurement. In order to fit within the full distance range, two exponential terms have to be used and the fit function is given by $I = I_0(e^{-x/\Lambda_L} + A \cdot e^{-x/\Lambda_S})$. For the fibre QA procedure the data points are fitted with an exponential function of the form $I = I_0 e^{-x/\Lambda}$ between 100 cm and 300 cm.

parameters, e.g. the energy deposited by a charged particle (or high energy photon) in the fibre core, the trapping efficiency of the fibre, the quality of coupling between fibre and photodetector or the photon detection efficiency of the latter.

In our set-up (see figure 5), electrons of 1.1 ± 0.1 MeV from an energy filtered Sr-90 radioactive source, which is based on a magnet and two collimators, are used. The electrons traverse a carefully aligned vertical stack of three scintillating fibres which are jointly read out by a single Silicon Photomultiplier (SiPM type Hamamatsu S13360-1350CS). The stacked geometry, as shown in figure 5, right, leads to an effective average path length of the electrons in the active fibre parts of 0.52 mm. It has been chosen to increase the signal amplitude (and therefore the S/N ratio), compared to a single fibre.

The fibres under test are approximately 2.6 m long. At one end, the three fibres were glued into a cylindrical plastic ferrule and then cut with a diamond milling tool in order to achieve a good quality end cut. The other end was left unmachined. Two fibres with the same diameter, placed on top and below the fibres under test, were read out individually by two Hamamatsu H7826 Photomultiplier Tubes (PMTs) and their coincidence defined the trigger for the readout. The trigger ensures that only electrons traversing all three test fibres were recorded. The SiPM signal was

2018 JINST 13 P10025

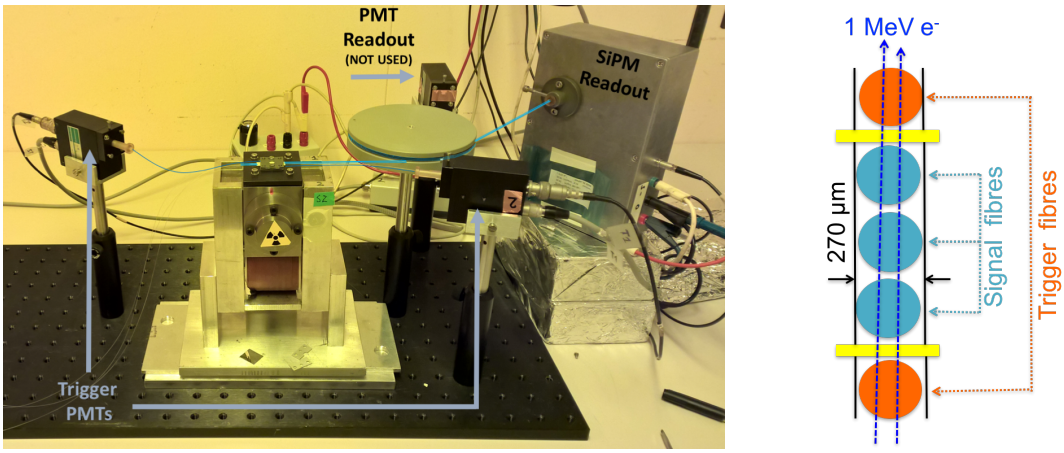

Figure 5. Left: picture of the experimental set-up used for light yield measurements. Right: details of the fibre arrangement on top of the electron gun. Thin sheets of opaque plastic serve as optical separation between the trigger fibres and the fibres under test.

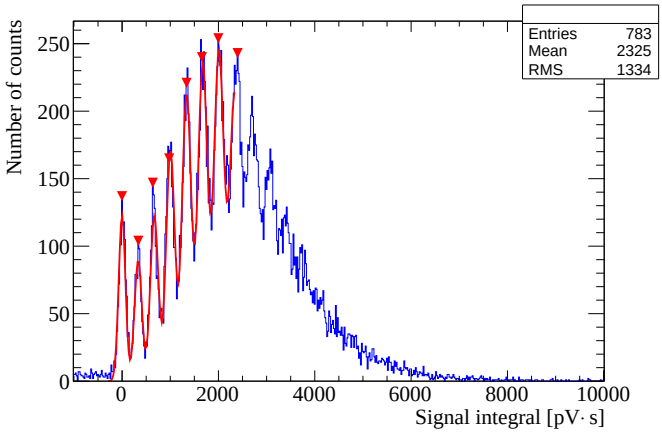

Figure 6. Example SiPM charge spectrum measured at a distance of 240 cm from the fibre end. The spectrum was fitted with multiple Gaussian functions (red line) to extract the charge corresponding to p.e. from the peak distances. The red markers indicate the peak positions found by the software. After appropriate pedestal subtraction, the mean charge can be converted to light yield in units of p.e.

read out with a digital oscilloscope (LeCroy WaveRunner 104MXi-A). Integration of the waveform $1/R \cdot \int V(t)dt$ with $R = 50\,\Omega$ being the impedance of the oscilloscope, leads to the signal charge Q, which is converted to the number of p.e. by means of the photoelectron peak structure provided by the SiPM. Figure 6 shows a typical charge spectrum taken with the Sr-90 source at a distance of 2.4 m from the readout end. Photoelectron peaks up to $N_{\mathrm{pe}} \approx 10$ are clearly visible. The set-up is placed in a temperature stabilised dark room. A more detailed description of the set-up and its components can be found in ref. [6].

In the beginning of the QA campaign, we measured the light output at distances $d = 90\,\mathrm{cm}$ to $d = 240\,\mathrm{cm}$ from the SiPM in steps of 30 cm. The data points fit to a single exponential function $f(d) = N_{\mathrm{pe}} e^{-d/\Lambda}$, which allows to extract the light yield by extrapolating to $d = 0$ and provides an

2018 JINST 13 P10025

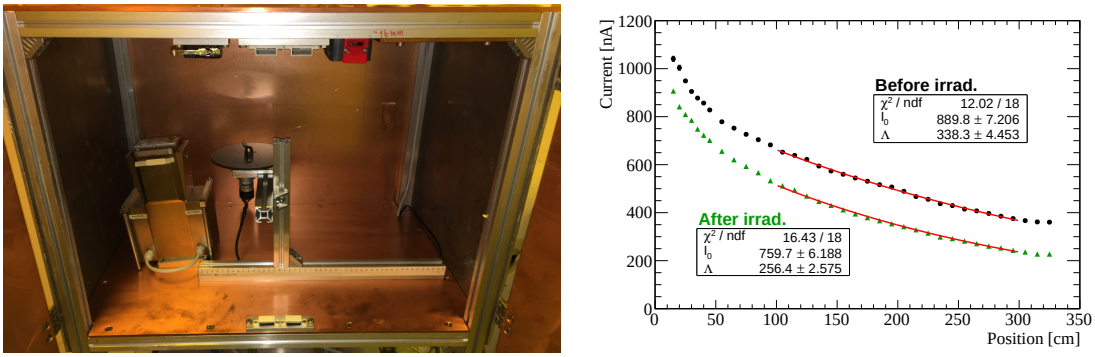

Figure 7. Left: X-ray set-up inside custom-made shielding box. Right: attenuation length measurement of a fibre sample from the main series production before and after irradiation with X-rays to a dose of 1 kGy. The mean energy of the X-rays was about 12 keV.

additional (but less precise) determination of the attenuation length Λ. The minimum acceptable value of the light yield at $d = 0$, agreed upon with the supplier, was 8 p.e. At a later stage, in order to reduce the effort, we performed measurements only at a single point corresponding to $d = 240$ cm, which is the most important point in view of the later use of the fibres in the SciFi detector.

3.3 X-ray irradiation

As outlined in section 2, the radiation tolerance of the fibres is a key requirement for the SciFi tracker. X-ray irradiations do however not allow to assess tolerance to high energy hadrons, as the damage and annealing mechanisms appear to be very different. In the context of this QA program, X-ray irradiations were used as a tool to discover potential material impurities or other irregularities in the production sequence.

An X-ray set-up (see figure 7, left, and ref. [7]), based on an X-ray tube equipped with a tungsten target and powered at 40 kV, allowed to irradiate 3.5 m long fibre samples to a dose of about 1 kGy in 45 minutes (at a dose rate of about 23 Gy/min). To achieve uniform irradiation, the fibre was wound on a 15 cm diameter plastic wheel with a groove, which is placed in the set-up such that the coiled fibre faces the beam outlet at a distance of about 5 cm and rotated at constant speed. Dosimetry was done using dosimetric films (Gafchromic HD-810). Following the exposure to X-rays, the radiation induced attenuation coefficient was measured: $\alpha_{\text{rad}} = \alpha' - \alpha_0$ where $\alpha_0 = \Lambda_0^{-1}$ is the intrinsic and $\alpha' = \Lambda'^{-1}$ is the attenuation coefficient after irradiation. The X-ray irradiated fibres show a rapid partial annealing within minutes to about 70% of the intrinsic attenuation length, while the complete annealing requires about 1 month. Figure 7, right, shows the measurement of the attenuation length for a fibre sample before and after irradiation, respectively.

3.4 Diameter and cladding quality

Given the substantial quantity of fibres needed to build the LHCb SciFi tracker and the tight performance constraints discussed above, a close-mesh test of the diameter and an approach which guarantees a pass rate of close to 100% was needed. Based on a prototype developed at the RWTH Aachen (Germany), a fibre scanner was built which allowed to measure the fibre diameter in sub-mm

2018 JINST 13 P10025

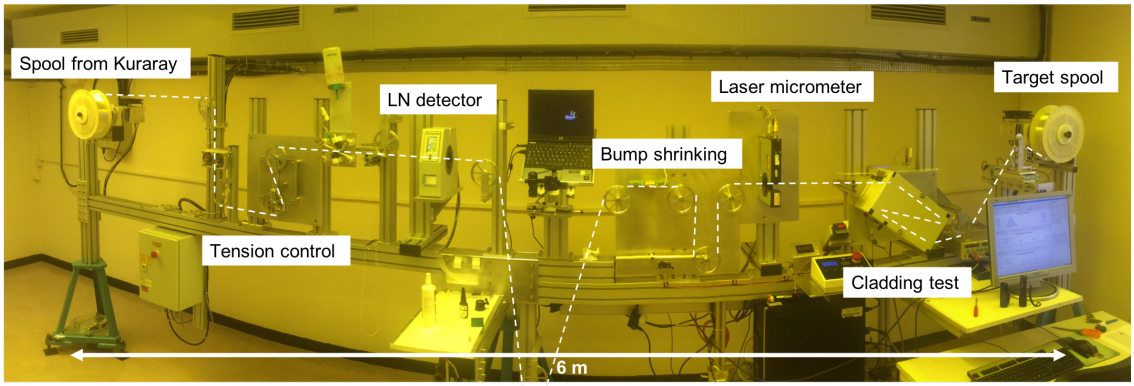

Figure 8. Picture of the fibre scanning machine at CERN.

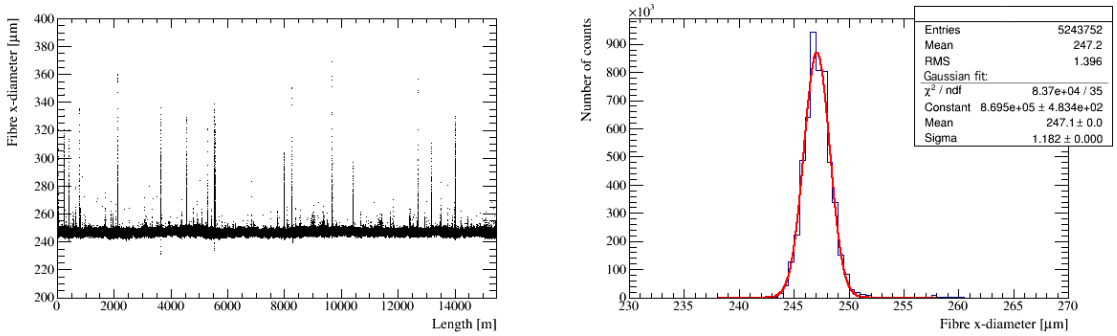

Figure 9. Measurement of the x-diameter along a fibre spool of 15 km total length. The histogram obtained from a projection on the vertical axis is fitted with a Gaussian to obtain the mean and sigma of the diameter for the corresponding spool. Much less than 1‰ of the fibre length is affected by bumps and therefore the diameter excesses are not visible in the histogram on the right hand side.

intervals for the full supply of 12,000 km. The second functionality of the machine is the effective neutralisation of fibre bumps with a diameter larger than 350 µm by an automatic hot shrinking procedure [8]. A further feature is an indirect assessment of the cladding quality along the full fibre length. The principle of the machine is summarised in figure 8, more details can be found in ref. [9].

The machine unwound the fibre from the source spool at a speed of about 1.2 m/s through two different laser micrometers (2-axis and 3-axis) to the target spool. While the speed of the rewinding spool was set to a user-defined fixed value, the speed of the unwinding spool was regulated by a fast feedback loop to maintain a constant fibre tension of 0.05 N, equivalent to 50 g. While the LN3015 provided a logic signal whenever the fibre diameter changes by more than ±25 µm, the AS5010 allowed for analog measurements (in two orthogonal directions x and y perpendicular to the winding direction) at a rate of 2.4 kHz.[3] The logic pulse of the LN3015 set the fibre speed to about 17 cm/s which corresponded to a diameter sampling step size of about 70 µm. Figure 9 shows the measured x-diameter along the length of a 15 km fibre spool. Figure 10 shows the correlation between x- and y-diameter for the same spool. In this context we defined the ovality of the fibre as

[3]BETA LaserMike LN3015 3-axis lump & neckdown detector, BETA LaserMike Accuscan AS5010 2-axis laser diameter gauge.

2018 JINST 13 P10025

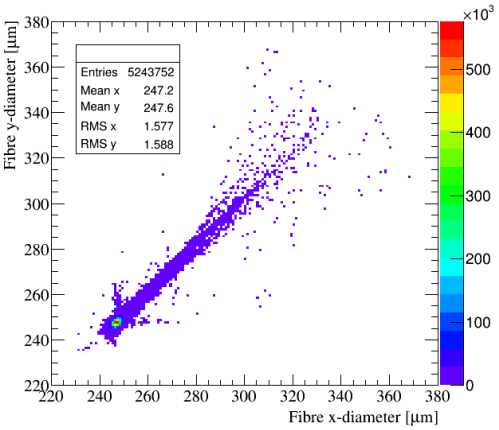

Figure 10. Correlation between x- and y-diameter for a 15 km fibre spool.

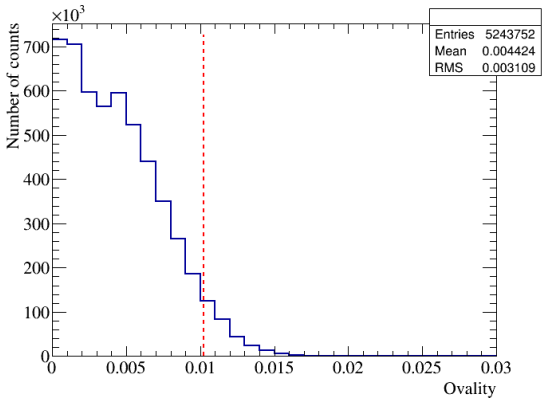

Figure 11. Ovality of a 15 km fibre spool. The red dashed line marks the 95% percentile with an ovality of about 1%.

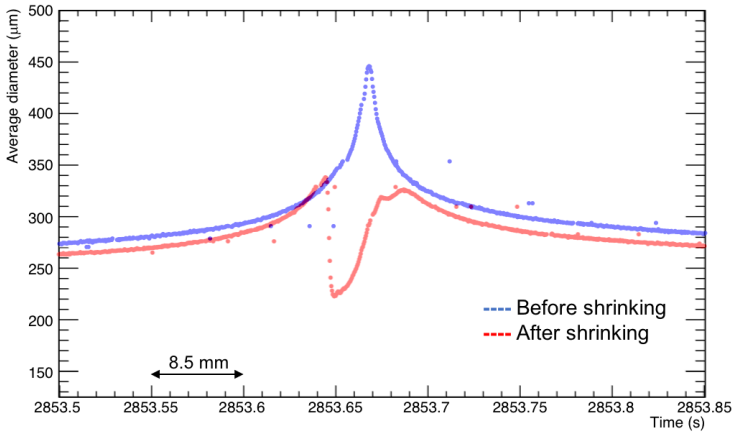

Figure 12. Illustration of bump shrinking. The untreated fibre has a bump which exceeds over a length of 6 mm the critical diameter of 350 µm. On the shrunk fibre the bump height is reduced to about 340 µm and a neck with a minimum diameter of 220 µm is formed.

$2 \cdot |x - y|/(x + y)$. It was agreed with the supplier that the 95% percentile of the ovality along a spool should not exceed 4% (see figure 11).

The slow motion is also the basis for the bump shrinking. Between the two laser micrometers, the fibre passes through a commercial wire drawing tool of 350 µm diameter which is maintained at a temperature of 100°C. Bumps with a diameter above 350 µm get stuck in the hot tool. The downstream motor continues to turn until a tension of 0.1 N (equivalent to 100 g) is reached. This tension, together with the elevated temperature, leads to a controlled deformation of the bump and pulls it through the tool, reducing its diameter to just 350 µm. This process takes typically a few seconds and works reliably up to bumps of about 500 µm size. To illustrate the bump shrinking process, figure 12 shows two different fibre sections, one untreated, the other after

2018 JINST 13 P10025

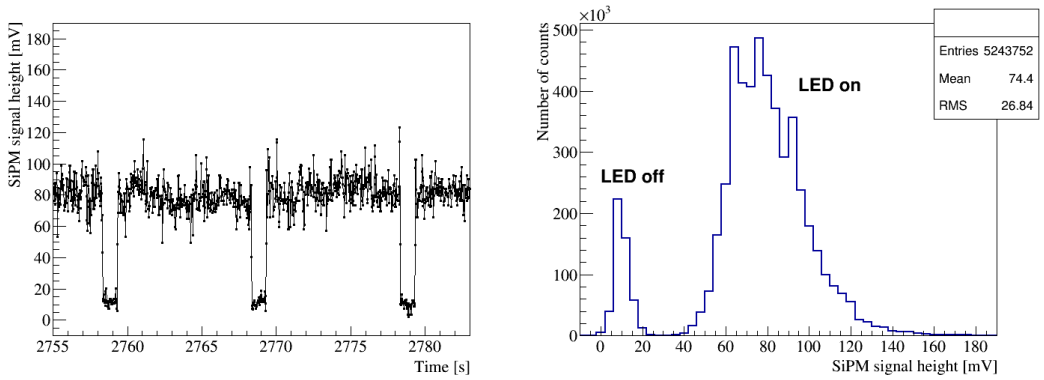

Figure 13. Left: time dependent SiPM signal, averaged every 0.01 s. Every 10 s the LED was switched off for 1 s. Right: SiPM pulse height histogram for a 15 km long fibre spool. Signal and background can be clearly separated. Monitoring the amount of light leaking out of the fibre along the full length gives information about the light transport properties.

passing the shrinking tool.[4] The light transmission across a shrunk bumpy fibre section is typically $\geq$ 85% [10]. Bumps significantly larger than 500 µm, which occur on average once per 10 km of fibre length, need to be cut out manually and the two fibre ends are spliced by means of a fast UV-curing optical adhesive.[5] Due to imperfect alignment and surface preparation of the two ends, the optical transmission across a glue joint is significantly reduced to values below 50%. Given the rarity of appearance, this will however not influence the overall performance of a full fibre mat.

The quality of the fibre cladding was assessed over its full length by passing the fibre over a length of about 1 m through a dark box. Shortly behind the entrance, the fibre was excited by a UV-LED (390 nm). About 70 cm downstream, a SiPM detector mounted in an integrating sphere, through which the fibre passes, measured the quantity of light leaking out of the fibre. Every 10 s the LED was switched off for 1 s, to monitor also the background signal detected by the SiPM (see figure 13, left). The significant light leakage was observable because over short distances light is efficiently transported by total internal reflections at the cladding/air interface. The signal was sampled at a rate of 2.4 kHz. It was therefore sensitive to local defects like bumps and diameter variations on mm to cm length scales, but also to variations of the attenuation length and the cladding quality on longer length scales. Figure 13, right, shows a typical histogram of the SiPM pulse height for a 15 km long fibre spool.

4 Additional measurements

In contrast to the systematic procedures described beforehand, the measurements reported in this section were not carried out on a regular basis. They were done mostly at the beginning of the fibre QA but also later in irregular time intervals and were meant to get in general a deeper understanding and better knowledge about the SCSF-78 fibres.

[4]The set-up does not allow to measure the very same bump before and after shrinking.
[5]Loctite 4305 LC.

2018 JINST 13 P10025

4.1 Spectral measurements

The emission spectrum of a scintillating fibre depends primarily on the choice of the wavelength shifter and on the distance between the excitation point and the photodetector. The set-up [5] used for the measurement of the emission spectrum and wavelength dependent attenuation length is the same as the one for the integral attenuation (see section 3), except that for spectral measurements the Si-PIN photodiode was replaced by a spectrometer (Ocean Optics USB2000+UV-VIS-ES). Figure 2 shows the emission spectra of the SCSF-78MJ fibre, excited at a distance of 15 cm, 95 cm and 295 cm from the spectrometer, with maxima in the blue wavelength region at about 440–460 nm. The data show clearly the aforementioned shifting of the emission spectrum towards longer wavelength when the distance between excitation and detection point increases, i.e. shorter wavelengths are more attenuated than longer wavelengths.

The spectral attenuation length was derived from exponential fits to the intensities measured with the spectrometer in wavelength bins of about 5 nm, at different excitation distances from the spectrometer. Again these fits were performed between 100 cm and 300 cm. The spectral attenuation length presented on the right in figure 2 shows that photons with longer wavelengths are less attenuated in the fibre, with the exception of the two minima at $\lambda \sim 535$ nm and $\lambda \sim 610$ nm. The enhanced absorption in these regions can be assigned to the excitation of high harmonics of the aromatic C-H stretching vibration levels of polystyrene [11].

4.2 Minimum bending radius

During storage on the spool, in the above described scanning operations and, finally, also during the winding process to fibre mats, the fibres are (temporarily) bent to various radii. If the bending exceeds the elastic limit of the core or cladding materials, small cracks may form and evolve in time, which eventually may lead to light scattering and losses, manifesting themselves in a reduced attenuation length.

Stability measurements were performed over periods of typically 2 to 4 days using the above described set-up (see section 3 and ref. [6]) which was originally conceived for the measurement of the ionisation light yield. In between the excitation point, where a set of three fibres was exposed to mono-energetic electrons from the Sr-90 source, and the light detection by the SiPM detector, the fibres were bent to the desired radius by passing them through a wound glass tube [12] or, for small radii, by simply winding them around a circular rod. Compared to excitation of the fibre with an UV-LED, the chosen approach has the advantage that the energy deposition in the fibre is highly stable in time, such that any observed reduction of signal amplitude can be attributed to a degradation of the fibre under bending. The light yield was measured in regular intervals (e.g. every hour) and investigated for trends in time.

The results of the measurements are shown in figure 14 for different bending radii. We observed no degradation of the light output for bending radii down to $r = 10$ mm. Going below that radius seems to damage the fibre and leads to light loss, indicating that the minimum bending radius is below 10 mm, which confirms that the fibres could not be damaged during the scanning operations (smallest wheel in fibre scanner has $r = 25$ mm). Especially for a bending radius of 4 mm it is clearly visible that there is a damage due to the initial bending of the fibre at $t = 0$, which leads to a significant reduction in light yield within the first few hours. Such an effect may be also visible in

2018 JINST 13 P10025

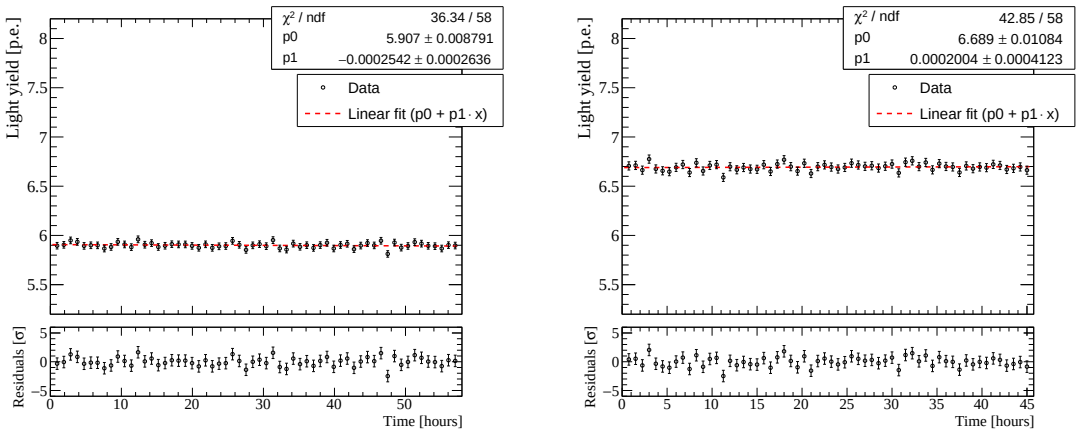

(a) $r = 15\,\mathrm{mm}$

(b) $r = 10\,\mathrm{mm}$

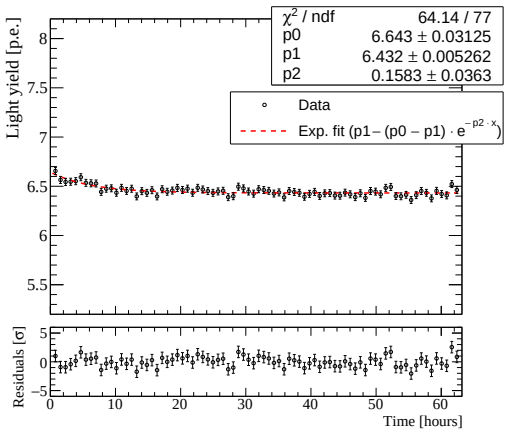

(c) $r = 6\,\mathrm{mm}$

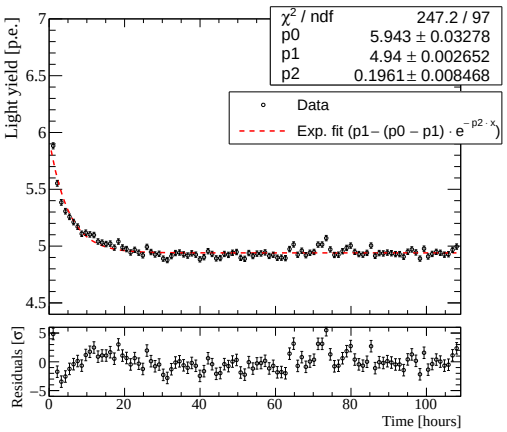

(d) $r = 4\,\mathrm{mm}$

Figure 14. Results of the bending tests. For bending radii $r = 15\,\mathrm{mm}$ and $r = 10\,\mathrm{mm}$ the slope is compatible with zero within the accuracy of the fit. For each measurement a new fibre sample was used and therefore the initial light varies.

the $r = 6\,\mathrm{mm}$ data, however less pronounced. After the initial loss we see almost no further change in the light yield, suggesting that a measurement time in the order of two days should be enough to see an effect due to bending.

4.3 Decay time

In order to measure the scintillation decay time of the fibre, a fast pulsed UV-LED (PicoQuant PLS370, $\lambda = 375\,\mathrm{nm}$, $\sigma \sim 220\,\mathrm{ps}$ pulse width) was placed at a distance of about 10–15 cm from one fibre end in order to laterally excite a single fibre. The fibre was machined with a diamond milling tool in order to achieve a good quality end cut and attached to a fast PMT (Hamamatsu H7826). The light intensity of the LED was adjusted such that the PMT detected primarily single

2018 JINST 13 P10025

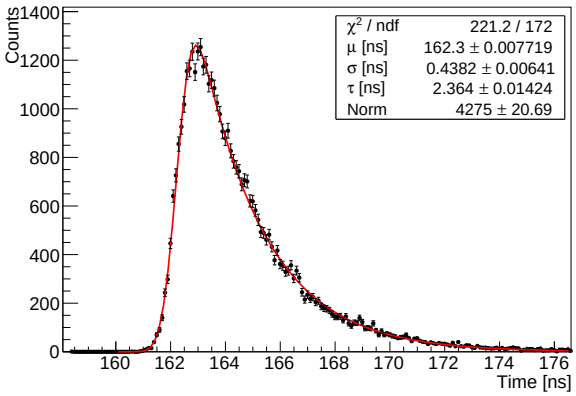

Figure 15. Time response of the SCSF-78MJ fibre following excitation with short LED pulses of $\lambda = 375$ nm.

photons. A pulse generator drove the LED and provided the start signal, whereas the amplified and discriminated (threshold 0.5 p.e.) PMT signal gave the stop signal for each single event. Data acquisition was done using a LeCroy WaveRunner 104MXi-A digital oscilloscope. The resulting time distributions were fitted with an exponential function containing the decay time constant τ of the scintillation light, convoluted with a Gaussian accounting for the overall time jitter of the experimental set-up, given by [13]:

$$f(x;\mu,\sigma,\tau) = \frac{1}{2\tau}\exp\left[\frac{1}{2\tau}\left(2\mu + \frac{\sigma^2}{\tau} - 2x\right)\right]\operatorname{erfc}\left(\frac{\mu + \frac{\sigma^2}{\tau} - x}{\sqrt{2}\sigma}\right) \tag{4.1}$$

where erfc is the complementary error function.

Figure 15 shows the measured and fitted time distributions for the SCSF-78 fibre. The decay time constants of 2.4 ns is slightly below the 2.8 ns provided in the Kuraray product catalog. The system time jitter was fitted to $\sigma \sim 450$ ps.

5 Natural aging

In the absence of ionising radiation, organic scintillators may still show a slow but continuous degradation of their optical parameters over time scales of years [14–16]. The LHCb SciFi tracker is foreseen to operate for about 10 years. Taking into account the construction phase, at the end of the experiments lifetime, the fibres will be about 14 years old. Even relatively small aging rates (e.g. 1%/year) may therefore have a significant impact on the detector performance.

Natural aging of plastic scintillators may result from a combination of phenomena like crazing (under stress), diffusion of small molecules (like water or oxygen) and oxidation, where the latter two phenomena depend on temperature and oxygen concentration. The aging results described below were obtained from attenuation length measurements performed on bare fibre samples. The reproducibility of these measurements was found to be about ±2%. Light yield repetition measurements were also performed. However, their precision is lower and in all cases the reduced signal at the fibre end could be explained by the reduced attenuation length only.

2018 JINST 13 P10025

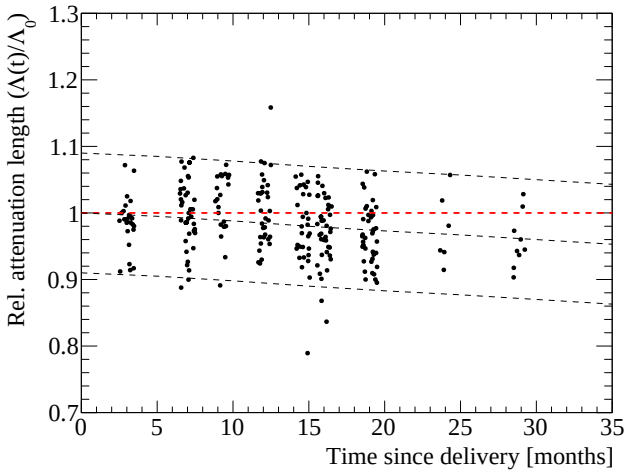

Figure 16. Attenuation length measured after a number of months normalised to the initial attenuation length at delivery. The time is smeared randomly by ±2 weeks, which is the typical time needed to process one batch. The black dashed lines are added to guide the eye. At the time of the measurement only a limited number of samples older than 20 months was available.

Between the initial measurement shortly after delivery and the repetition measurement, the samples of typically 3.5 m length were kept in conventional household plastic bags and stored in ambient air in a fully dark and temperature controlled room ($T = 22 \pm 1°\mathrm{C}$). The repetition measurement cover a period in time of 30 months with respect to the delivery date.

In analogy to damage by radiation, the degradation of the attenuation length is described by an additional damage factor α_{O_2}, which is derived from $\alpha_{O_2}(t) = \alpha(t) - \alpha_0$, with $\alpha = 1/\Lambda$. Λ_0 is the initial attenuation length of a fibre sample at its delivery. The fibre production date is typically 1–2 months before delivery. No effort was made to investigate the precise production date of every individual spool.

Figure 16 shows the attenuation length for all tested fibre samples measured at a number of months since delivery, normalised to the initial attenuation length Λ_0. The distribution has a small negative trend, i.e. the attenuation length degrades slowly. This becomes also clear when looking at figure 17, which depicts the correlation between the additional attenuation α_{O_2} and the initial attenuation length Λ_0 for different measurement times. In general it seems that initially high attenuation length fibres tend to degrade, while fibres with initially low attenuation length even show a positive α_{O_2}, i.e. their attenuation lengths improve with time. However, after a certain time (about 15 months) the positive trend is over and the fibres just degrade. The reason for this behaviour is not fully understood. Possibly there is an additional phenomenon which competes with the oxidation of the polystyrene, as for instance relaxation of mechanical stress introduced during the fibre production.

By calculating the average α_{O_2} of all samples measured after the same time since delivery, the left plot in figure 18 is obtained. Up to 15 months, there is no clear trend because, in first approximation, positive and negative effects compensate each other. For times above 15 months a clear correlation between additional damage and time since delivery is observed, which can again

2018 JINST 13 P10025

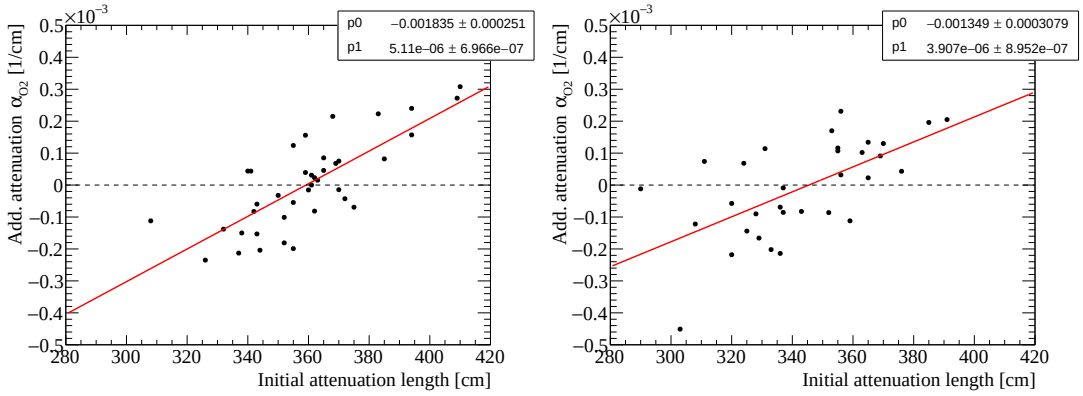

(a) After 7 months. **(b)** After 12 months.

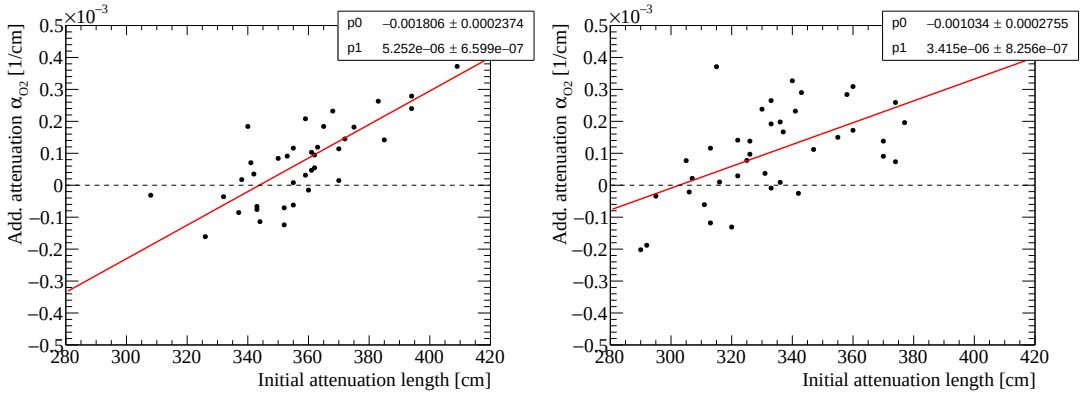

(c) After 16 months. **(d)** After 19 months.

Figure 17. Correlation between additional attenuation α_{O_2} and initial attenuation length at delivery for four different measurement times with respect to the delivery date.

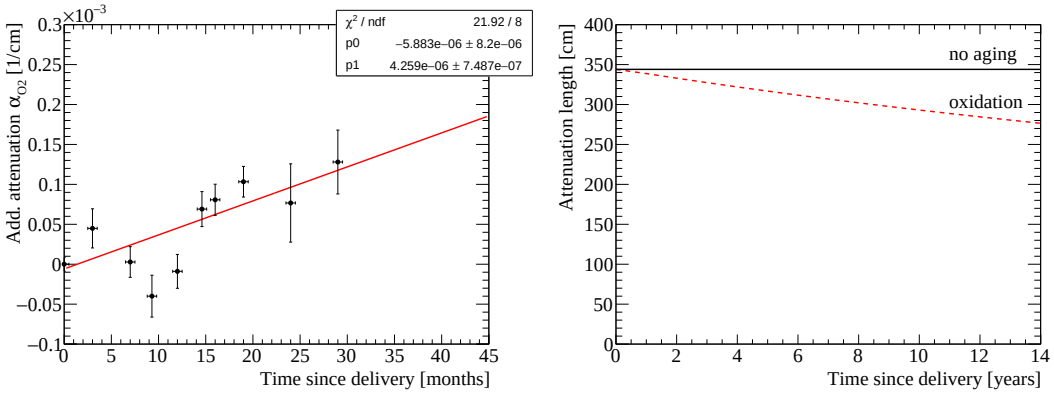

Figure 18. Left: additional attenuation α_{O2} for different measurement times with respect to the delivery date. The vertical error bars scale with the sample size n as $1/\sqrt{n}$. The horizontal error bars are set to ±2 weeks, which corresponds roughly to the time needed for one shipment to be processed. Right: extrapolation of the attenuation length until the end of the scheduled life time of the SciFi tracker based on a linear extrapolation of α_{O_2}.

2018 JINST 13 P10025

in first approximation be described as linear. This allows to extrapolate the attenuation length of fibres until the end of the planned life time for the SciFi tracker, as shown on the right hand side of figure 18. The calculation results in an aging rate of about 1.4% per year.

The hypothesis of a continuous aging of the fibres will be continually assessed over months and years to come by repeated measurements of the stored samples, probably in intervals of 3 months. As for any chemical reaction it should be possible to accelerate the reaction rate k by increasing the temperature or by increasing the concentration of the reaction partner: $k = f(T, [O_2])$. The Kuraray team is therefore performing accelerated aging measurements at elevated temperature (e.g. 40, 50 and 60°C) on 1 mm fibre samples which are easier to handle and measure than 0.25 mm ones. Assuming a linear increase of the damage factor in time $\alpha_{O_2} = k \cdot t$ and expecting k to follow an Arrhenius law $k = k_0 \cdot \exp\left(\frac{-E_a}{R \cdot T}\right)$, a plot of $\ln k$ versus $1/T$ allows to determine the activation energy E_a of the reaction and allows then to predict the damage factor at any temperature.

In the SciFi tracker, once processed to fibre mats, the fibres are surrounded by a few tens of µm thick layer of epoxy glue loaded with about 10% TiO_2. The top and bottom surface of the fibre mat are covered by kapton films of 20 µm thickness. For the time being, attenuation length and light yield measurements on a fibre mat with a precision in the percent range are very hard to achieve. It is therefore unclear whether fibres inside a fibre mat show a different (hopefully lower) aging rate than the bare fibre samples.

6 Results and discussion

In this section we discuss the most important results of the quality assurance measurements for the total production volume of 12,000 km of fibres.

Attenuation length. The large fibre length of 240 cm in the SciFi tracker makes the attenuation length a key parameter, for which a lower acceptance limit of 300 cm was agreed with the supplier. Fibre samples of 3.5 m length were taken from every of the about 950 spools and analysed as described in section 3. Also Kuraray took samples from every spool and analysed them on a set-up which is based on the same measurement principle, however the light from the fibre was detected by a photomultiplier tube, which has a more blue-peaked spectral sensitivity than our PIN-diode. From a simple model, folding the spectra of fibre emission and photodetector sensitivity one expects that the Kuraray attenuation length values are approximately 10% shorter than the ones measured with the CERN set-up. Furthermore, the values provided by Kuraray represent averages of several measurements performed on the same fibre sample.

Figure 19, left, shows the histograms of all performed attenuation length measurements, both at CERN and at the supplier. In view of the aging observations described in the previous section, it should be noted that the measurements at CERN and at the supplier could have been made with a delay of several months. The mean value of the CERN measurements of the attenuation length is 350 cm, about 2.6% higher than the Kuraray values of 341 cm. The histogram of the Kuraray measurements has a smaller standard deviation (14.7 cm compared to 22 cm), which may be due to the fact that it is based on averaged measurements. The right hand side of figure 19 shows the time evolution of the attenuation length over the full production time of almost 2 years. For this plot, averages of all spools (typically 24) of one shipment were calculated. Apart from an initial increase

2018 JINST 13 P10025

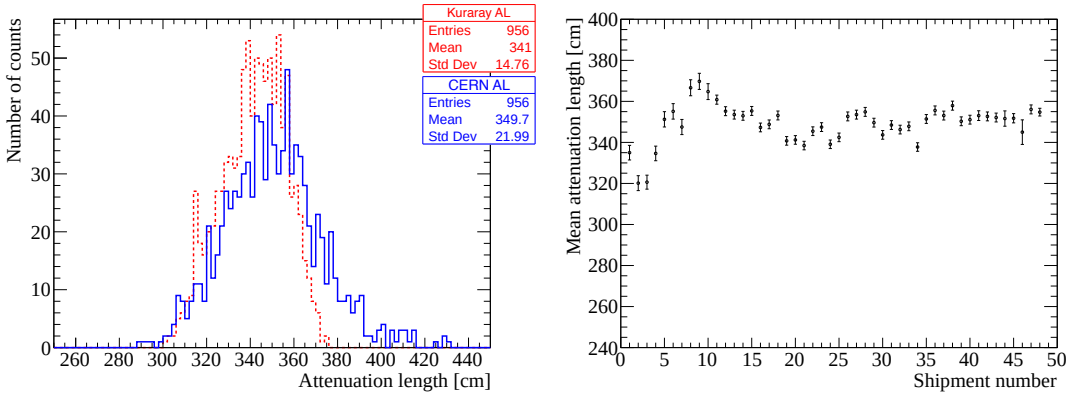

Figure 19. Results of attenuation length measurements for all tested samples. Left: comparison Kuraray (red dashed) and CERN (blue) measurements. Right: CERN measurements averaged per shipment.

of the attenuation length during the pre-series and early main-series production, the attenuation length was very constant throughout the full production and well above the acceptance limit.

Light yield. Similar to the attenuation length, the scintillation light yield of the fibre has a crucial impact on the final detector performance, in particular the hit efficiency which is a key number for any tracking detector. As part of the QA, we initially measured the light yield of only a subset of the fibre spools. The measurement of six data points along the fibre and the exponential extrapolation to zero distance was too time consuming to perform it for all spools. At a later stage it was decided to measure only the light yield at a distance of 240 cm from the photodetector, however this measurement was then performed for all spools. The new approach had the advantage that we could select the spools with the highest light yield and reserve those for the production of the SciFi beam pipe modules which will later on be exposed to the highest radiation levels. The minimum acceptance limit of 8 p.e. at 0 cm, as agreed with the supplier, corresponds to about 4 p.e. at 240 cm (assuming an attenuation length of 350 cm). The left plot of figure 20 shows the time evolution of the light yield measured at 240 cm. The ramp up of the attenuation length observed during the pre-series, is also reflected in the light yield. Otherwise, the light yield was very stable around a mean of about 6.8 ± 0.5 p.e., as the histogram on the right shows, and at any time exceeded the acceptance limit.

X-ray irradiation. As explained in section 3.3, the X-ray irradiation test was meant as an additional tool to detect material impurities or other irregularities in the production process. We typically measured 1-2 samples from every shipment (typically 24 spools). As shown in the left plot of figure 21, the exposure to 1 kGy of X-ray irradiation led on average to a reduction of the attenuation length by 25%. The plot on the right side shows the identical data expressed as additional attenuation factor α_{rad} which was found to lie around $1 \cdot 10^{-3}\text{cm}^{-1}$. None of the measurements hinted at any anomalies.

Geometry. The full supply of 12,000 km of fibres passed the fibre scanner described in section 3.4. From the recorded scan data (stored in ROOT files), the fibre diameter (mean and sigma in two

2018 JINST 13 P10025

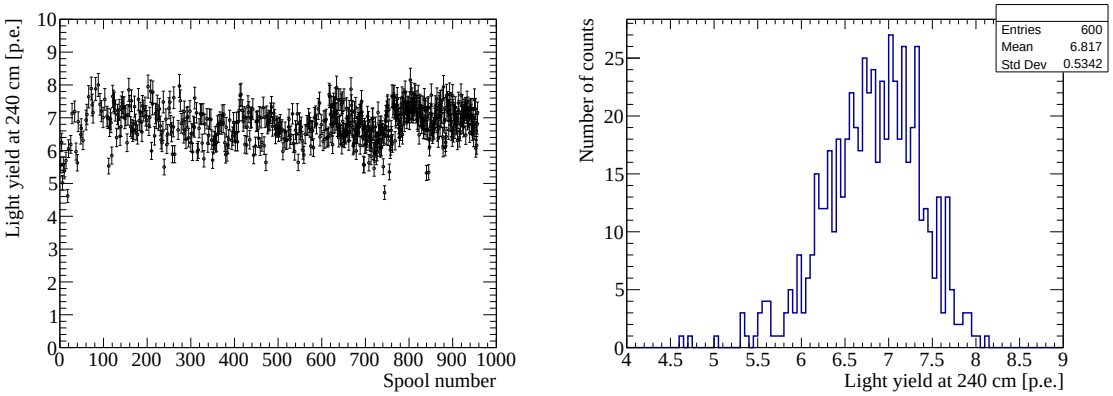

Figure 20. Results of light yield measurements for all tested samples. Light output is measured at a distance of 240 cm from the SiPM. Right: projection on y-axis.

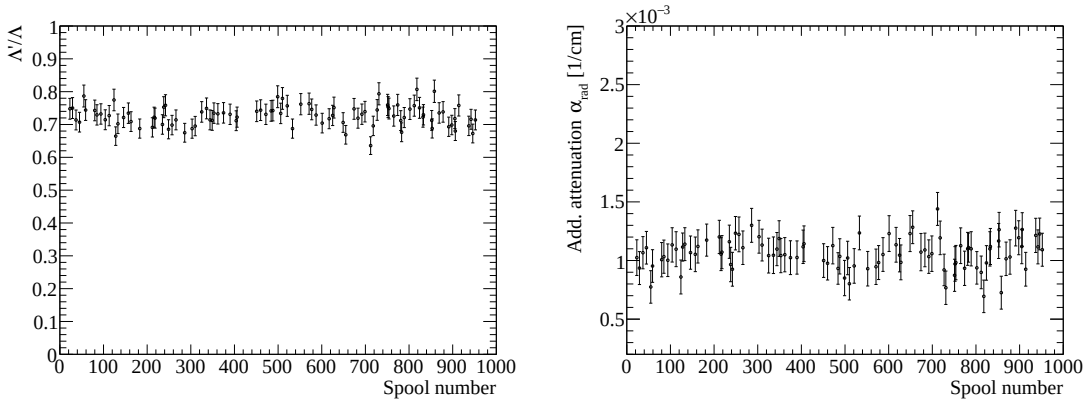

Figure 21. Results of X-ray irradiation tests for all tested samples. Left: reduction of the attenuation length. Right: radiation induced attenuation coefficient.

projections), the ovality and the number of bumps exceeding 350 µm, before and after the shrinking process, were extracted.

The histogram in figure 22, left, shows the mean diameter of (almost) all spools in comparison with the values provided by the supplier. For the CERN measurements, both projections are shown. The data reveals a systematic calibration offset of about 2.5 µm, which was constant throughout the full production. The plot on the right hand side shows that the ovality of the fibres was on average 1% with a tail to about 3% and just two spools at an ovality of about 4%.

Figure 23 shows the sigma of the fibre diameter per spool, averaged over all fibres of a shipment. Starting with an initial sigma of 1.6 µm, the quality of the fibre improved in the second half to about 1.3 µm. At the same time, and in phase with this improvement, also the number of bumps exceeding a diameter of 350 µm went from initially 8 per spool down to 5-6 per spool for the last few shipments, with an average over the full production of about 7 (see figure 24, left).

The bump shrinking procedure allowed to remove most of these bumps in a fully automated manner. From the average of 7 bumps per spool, 0.5 were left after shrinking or cutting. Practically

2018 JINST 13 P10025

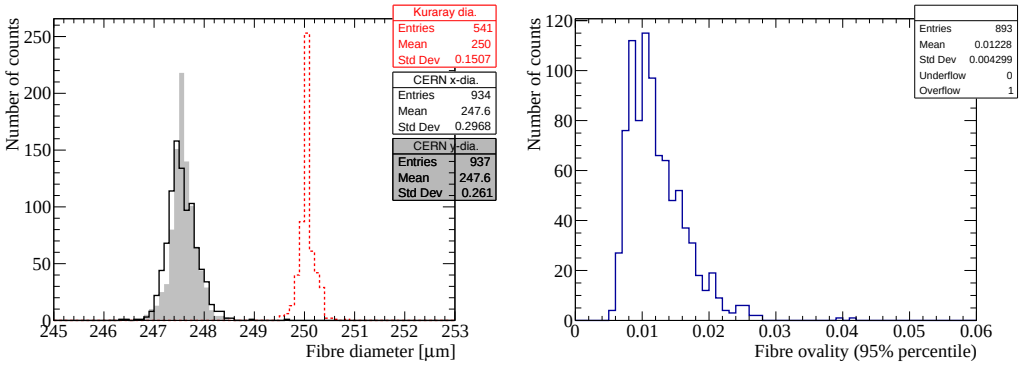

Figure 22. Results of diameter scans for all processed spools. Diameters along the two axes measured at CERN and average diameter as given by Kuraray (red dashed) on the left. Fibre ovality for all scanned fibre spools on the right hand side.

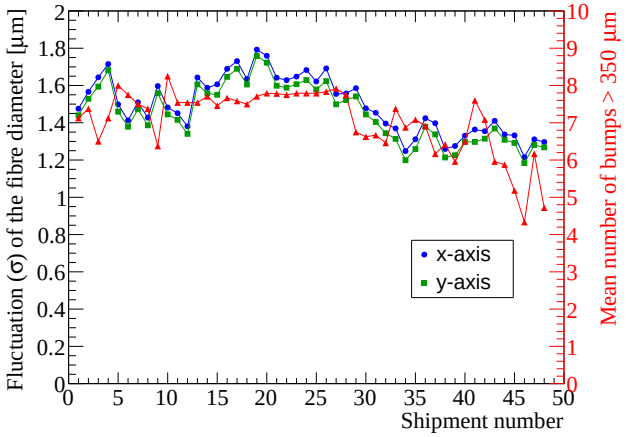

Figure 23. Average Gaussian σ of the diameter histogram for every shipment and average number of bumps larger than 350 µm per spool before bump shrinking in red (given by Kuraray). For clarity the values of all spools from one shipment are averaged.

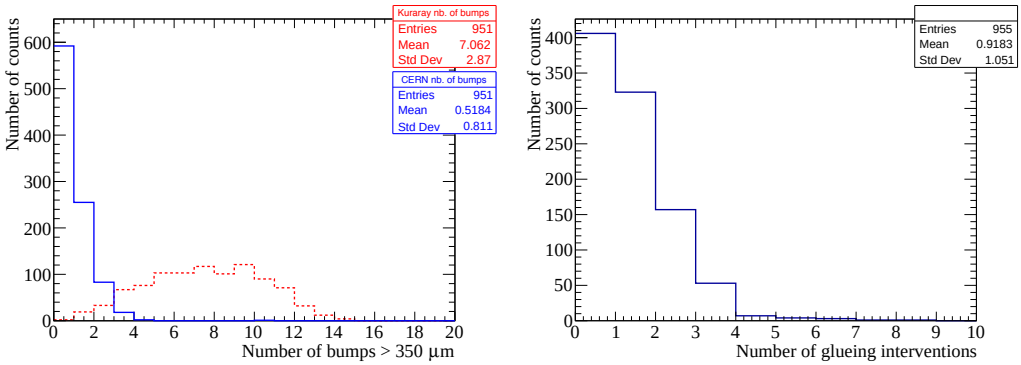

Figure 24. Left: number of bumps with a diameter larger than 350 µm per spool measured by Kuraray (red dashed) and after bump shrinking at CERN (blue solid). Right: number of manual glueing interventions per spool.

2018 JINST 13 P10025

all these remaining bumps have sizes just slightly above 350 µm and have posed no problems during fibre mat winding. The number of manual cut and glue interventions for bump sizes above 500 µm was less than 0.9 per spool. An experienced operator needed about 10–15 minutes for this intervention, while the typical scanning time of a spool (12,500 m) was about 3.5 h.

7 Summary and outlook

Over a period of almost two years a total of 12,000 km of double-cladded scintillating fibres of type SCSF-78 with a diameter of 0.25 mm were tested for their suitability in the LHCb SciFi tracker upgrade.

The fibres were delivered in bi-weekly intervals, wound on 956 spools with nominal lengths between 10,000 and 15,000 m. The fibres were found to be of high quality for all assessed optical and geometrical parameters and clearly exceeded the minimal acceptance criteria. Apart from a ramp-up during the pre-series phase (500 km) the quality showed only little variations over the full period.

A total of 3 spools were rejected and replaced by the supplier as they showed diameter variations on the level of up to ±25 µm on length scales of a couple of meters and also elliptic deformations. The intrinsic production yield was therefore 99.7%.

The fibre scanning machine with its specifically developed bump shrinking device turned out to be a key tool, which provided not only highly granular and precise information on fibre diameter and ovality, but also allowed to refine the quality of the fibres by eliminating effectively all bumps exceeding a diameter of 350 µm. This achievement has greatly facilitated the winding of fibres to 6-layer mats. No mat had to be rejected at any of the four mat winding centres in the SciFi project because of flaws in the winding pattern which were due to fibre bumps.

Typically, the QA of a complete shipment was completed within 2 weeks after arrival at CERN. This tight schedule was meant to minimise the production of 'bad' fibres before a process problem would have been detected.

The completion of this large QA task in time and well beyond the contractual performance was only possible due to an efficient communication and coordination with the Kuraray technical and commercial teams. It is worthwhile to mention that all 48 shipments left the company in Japan on precisely the days which the supplier had communicated prior to the start of the production. Occasional delays of a few days were exclusively due to logistics and custom problems in Geneva.

In view of the natural aging phenomena described in section 5, the fibre quality, in particular the attenuation length, of a sub-set of the samples will be re-measured in 3-months intervals in order to allow for a reliable prediction of the effect to be expected over the planned lifetime of the LHCb SciFi tracker. We expect to complement this information with accelerated aging results currently performed at Kuraray.

Acknowledgments

This research was carried out through the participation of the authors, except O. Shinji, in the CERN LHCb collaboration. We would like to express our gratitude to our technical staff at CERN and the RWTH Aachen (Germany), in particular to P.A. Giudici, F. Granier, G. Pierschel, X. Pons, T. Schneider and M. van Stenis for their continuous competent support during the construction and operation

2018 JINST 13 P10025

of the fibre scanning machine. Many thanks to Mika Väänänen and Šejla Hadžić who worked with us as CERN summer students (2017 and 2018). We would also like to acknowledge the high level of competence and professionalism of the technical and commercial teams at Kuraray. L. Gavardi acknowledges the support of the Deutsche Forschungsgemeinschaft (DFG, Emmy Noether programme: AL 1639/1-1). L. Gruber acknowledges the support of the Marie Skłodowska-Curie Fellowship Programme as part of the EU-funded project "Cofunding of the CERN Fellowship Programme (COFUND-FP-CERN-2014)". Last but not least, our thanks go to A. Schopper and U. Uwer (University of Heidelberg, Germany) for their continuous interest and support in the fibre QA task.

References

[1] LHCb collaboration, *LHCb Tracker Upgrade Technical Design Report*, CERN-LHCC-2014-001.

[2] C. Joram, G. Haefeli and B. Leverington, *Scintillating Fibre Tracking at High Luminosity Colliders*, 2015 *JINST* **10** C08005.

[3] R. Ekelhof, *Studies for the LHCb SciFi Tracker. Development of Modules from Scintillating Fibres and Tests of their Radiation Hardness*, CERN-THESIS-2016-098.

[4] O. Borshchev, A.B.R. Cavalcante, L. Gavardi, L. Gruber, C. Joram, S. Ponomarenko et al., *Development of a New Class of Scintillating Fibres with Very Short Decay Time and High Light Yield*, 2017 *JINST* **12** P05013.

[5] C. Alfieri, A.B. Cavalcante and C. Joram, *A set-up to measure the optical attenuation length of scintillating fibres*, CERN-LHCb-PUB-2015-011.

[6] C. Alfieri, A.B. Cavalcante and C. Joram, *An experimental set-up to measure Light Yield of Scintillating Fibres*, CERN-LHCb-PUB-2015-012.

[7] L. Gavardi, A.B. Cavalcante, C. Joram and R. Kristic, *A setup to perform X-ray irradiation tests on scintillating fibres for the SciFi project*, CERN-LHCb-PUB-2017-008.

[8] A.B. Cavalcante et al., *Shrinking of bumps by drawing scintillating fibres through a hot conical tool*, CERN-LHCb-PUB-2016-010.

[9] A. Bachlechner et al., *Scanners for the quality control of scintillating plastic fibres*, CERN-LHCb-PUB-2015-009.

[10] A.B. Cavalcante, L. Gavardi and C. Joram, *Quality of scintillating fibres after hot bump shrinking*, CERN-LHCb-PUB-2016-009.

[11] T. Kaino, M. Fujiki and S. Nara, *Low loss polystyrene core optical fibers*, *J. Appl. Phys.* **52** (1998) 7061.

[12] L. Gavardi, L. Gruber, C. Joram and M. Väänänen, *Measurement of the Minimum Bending Radius of Small Diameter Scintillating Plastic Fibres*, CERN-LHCb-PUB-2018-008.

[13] C.M. Hawkes, M. Kuhlen, B. Milliken, R. Stroynowski, E. Wicklund, T. Shimizu et al., *Decay Time and Light Yield Measurements for Plastic Scintillating Fibers*, *Nucl. Instrum. Meth.* **A 292** (1990) 329.

[14] H. Blumenfeld and M. Bourdinaud, *Aging of plastic scintillating fibers*, *Appl. Opt.* **31** (1992) 2791.

[15] V. Senchishin et al., *New Radiation Stable and Long-Lived Plastic Scintillator for the SSC*, FERMILAB-TM-1866, 1993.

[16] A. Artikov, J. Budagov, I. Chirikov-Zorin, D. Chokheli, M. Lyablin, G. Bellettini et al., *Properties of the Ukrainian polystyrene-based plastic scintillator UPS 923A*, *Nucl. Instrum. Meth.* **A 555** (2005) 125.

2018 JINST 13 P10025